# Agrégation et dispersion de la fraction inférieure à 2-µm des luvisols

Article publié dans Soil Sciences Society of America Journal (2015)

**Van den Bogaert, R.**[1], Labille, J.[2], Cornu, S.[1]

*1- INRA, UR 1119 Géochimie des Sols et des Eaux, F-13100 Aix en Provence, France.*

*2- Aix-Marseille Université, CNRS, IRD, CEREGE UMR 7330, F-13545 Aix en Provence*

## V.1. Résumé (français)

La migration des particules inférieures à 2 µm dans les pores du sol est responsable du transfert préférentiel de contaminants variés et de la différentiation texturale des luvisols. Les mécanismes d'agrégation et de dispersion des particules argileuses sont supposés avoir un rôle majeur dans ce processus de migration. Cependant, ces mécanismes ont principalement été étudiés sur des minéraux argileux purs et bien cristallisés plutôt que sur des particules d'origine pédogénétique et souvent dans des conditions physico-chimiques peu représentatives des conditions du sol. Nous avons étudié l'impact respectif du pH et de la concentration en calcium sur l'agrégation et la dispersion de particules argileuses issues d'un luvisol sous des conditions représentatives de la solution du sol. Des approches statiques et dynamiques ont été suivis pour étudier les interactions entre particules sous l'effet de changements transitoires de la physico-chimie de la solution. A partir de ces expérimentations, nous avons dressé un diagramme de phase des argiles du sol en fonction de la concentration en calcium et du pH et nous avons identifié les mécanismes associés avec la formation de ces différentes phases. Nous observons que les particules issues de sol se comportent de façon similaire aux particules modèles, en ce sens que leur comportement est influencé par le pH et la concentration en calcium. L'effet de ces deux paramètres est couplé, et favorise l'agrégation lorsque la concentration en calcium est élevée et / ou lorsque le pH est faible. Ces effets sont réversibles sur une durée de temps correspondante à celle de l'infiltration de l'eau de pluie dans les macropores, à l'exception de la dispersion des particules induite par la dilution de la solution du sol. En resituant ces mécanismes physico-chimiques par rapport à la chimie des eaux de pluie et de la solution de sols, tirées d'une revue de la littérature, nous avons établi le rôle de ces mécanismes dans le transport de particules dans l'eau circulant dans la macroporosité.

Published December 1, 2014



# Aggregation and Dispersion Behavior in the 0- to 2-μm Fraction of Luvisols

**Romain Van Den Bogaert**
INRA
UR 1119 Géochimie des Sols et des Eaux
F-13100 Aix en Provence France

**Jérôme Labille***
Aix-Marseille Univ.
CNRS
IRD
CEREGE UMR 7330
F-13545 Aix en Provence France

**Sophie Cornu**
INRA
UR 1119 Géochimie des Sols et des Eaux
F-13100 Aix en Provence France

**The migration of particles smaller than 2 μm in soil pores is responsible for the preferential transfer of various contaminants and for soil textural differentiation in Luvisols. Aggregation vs. dispersion mechanisms of clay particles are suspected to play a major role in this migration process. However, these mechanisms have mostly been studied with respect to pure and well-crystallized clay minerals rather than pedogenetic particles and have often been performed under physicochemical conditions, which are poorly representative of soil conditions. We studied the respective impacts of pH and Ca concentration on aggregation and dispersion behavior of clay particles in a Luvisol under conditions encountered in the soil solution. Both static and dynamic approaches were followed in studying particle interactions and dynamics under transient phenomena. Based on these experiments, we have drawn a phase diagram for soil clays as a function of pH and Ca concentrations and have identified mechanisms associated with the formation of these different phases. We find that soil particle behavior in suspensions is similar to that recorded for model clays in that they are driven by both pH and Ca concentrations. These two parameters are interrelated and tend to favor aggregation at higher Ca concentrations and/or lower pH. These effects are reversible over the gravitational water time scale, with the exception of dilution-induced dispersion. In situating these physicochemical mechanisms within a literature review of rainwater and soil solution chemistries, we determine the expected role of these mechanisms on the transport of particles in gravitational soil water.**

Abbreviations: CCC, critical coagulation concentration; *I*, scattered intensity; *q*, wave vector; SEM, scanning electron microscopy.

Particle migration in soil is responsible for: (i) the preferential transfer of various contaminants bound to surfaces (Amrhein et al., 1993; de Jonge et al., 1998, 2004; Jacobsen et al., 1997; Laegdsmand et al., 1999; Ryan et al., 1998), notably pesticides, microbes, pathogen viruses, and heavy metals and (ii) lessivage—or argilluviation—which is defined as significant particle migration (Mercier et al., 2000) from a departure upper soil E-horizon (eluviated) to an accumulation Bt-horizon (illuviated) at the subsurface at the pedogenesis time scale. The latter phenomenon is the major pedogenetic process for Acrisols, Alisols, Albeluvisols, Lixisols, Luvisols, and Solonetz formations of the World Reference Base (WRB) soil classification (Bockheim and Gennadiyev, 2000; FAO, 2006). It also serves the pedogenetic process involved in the formation of Argid of Aridosol subgroups, Molisols, Oxisol kandic groups, and Spodosol alfic subgroups of the soil taxonomy classification (Bockheim and Gennadiyev, 2000; Soil Survey Staff, 1998).

Soil Sci. Soc. Am. J.
doi:10.2136/sssaj2013.12.0538
Received 20 Dec. 2013.
*Corresponding author (labille@cerege.fr).

Particle migration in soil decomposes over three stages: dispersion, transport, and fixation. Though numerous physical and physicochemical mechanisms drive these steps (Kaplan et al., 1993; Le Bissonnais, 1996; Le Bissonnais et al., 1989; Michel et al., 2010; Ryan and Elimelech, 1996; Ryan et al., 1998; Shang et al., 2008), their respective contributions are poorly understood. It is widely known that variations in aqueous environment physicochemical parameters modify interparticle forces and, thus, relative dispersion or aggregation of colloidal materials. Notably, the stability of suspended particles is closely related to particle surface charge properties, which vary depending on the ionic strength and pH of the solution, the counter-ion type, and the organic matter adsorbed on particle surfaces (Goldberg and Glaubig, 1987; Goldberg and Forster, 1990; Chorom and Rengasamy, 1995; Abend and Lagaly, 2000; Tombacz and Szekeres, 2004; Furukawa et al., 2009; Séquaris, 2010). In the case of clay particles, interactions are complicated by their lamellar morphology, resulting in the development of a permanent anionic charge on the basal surface and a variable charge (amphoteric sites) on the broken edges (Johnston and Tombacz, 2002; Tournassat et al., 2003). These particularities of clay particles result in various aggregation modes depending on the contributing surface charge (Hofmann, 1961; Van Olphen, 1977). Electrolyte and pH concentrations have an interrelated effect (Tombacz and Szekeres, 2004; Borgnino, 2013), as they simultaneously influence clay suspension behavior. The majority of these results were obtained through experiments on pure and well-crystalline clay minerals (bentonite of volcanic or hydrothermal origin, for example), which are considered here as model minerals. However, soil particles have a more complex mineralogical composition, are smaller in size, and exhibit poorer crystallinity levels and a higher number of defects, which may affect their reactivity (Goldberg and Forster, 1990; Liu et al., 1998; Elsass, 2005). Thus, the results obtained for model clays may not be directly applicable to soil minerals.

Moreover, the majority of stability experiments conducted on model clay have been performed under ionic concentration, pH, and suspended solid content conditions, which are relatively different from conditions that are typically encountered in soil solutions. Second, eluviated particles collected at the bases of soil columns or lysimeters are typically released within the first hour after a rain event (Laubel et al., 1999; Schelde et al., 2002; Majdalani et al., 2008; Vendelboe et al., 2011), which corresponds to the time scale of gravitational water infiltration. To our knowledge, this time scale and these specific physicochemical conditions have rarely been considered together in previous stability experiments. Thus, results obtained under such experimental conditions may not reflect processes that occur in soils.

The aim of the present work was to determine the contribution of physicochemical mechanisms during argilluviation processes. We thus examined (i) particle fractions smaller than 2 μm in a Luvisol (FAO, 2007), as this soil group is orthotypic to argilluviation; (ii) physicochemical conditions encountered in soils (pH, Ca concentration, and solid content [Cornu et al., 2014]); and (iii) a duration typical of the percolation time for gravitational water (1–5 h). The dispersion and aggregation dynamics of the soil colloids were monitored by laser diffraction. We aimed at determining (i) whether model minerals are representative of soil mineral stability; (ii) soil suspension stability levels following a rain event; and (iii) proposing fate scenarios for clay particles driven by physicochemical mechanisms within typical soils undergoing argilluviation.

## MATERIALS AND METHODS

### Studied Material

The studied soil fraction (smaller than 2 μm), which is hereafter called *lutum* (Stichting voor Bodemkaartering, 1965), was extracted from a Luvisol E-horizon that was already used for soil column experiments by Cornu et al. (2014). This fraction is composed mainly of smectite illite, kaolinite, chlorite, and quartz (Cornu et al., 2014).

To extract a fraction smaller than 2 μm, 50 g of soil was dispersed in 1 L of ultrapure water and sonicated for 20 min at 47 kHz and 35 W. Labile organic matter was then oxidized through the addition of 40 mL of $H_2O_2$ (30%) and after subsequent heating of the suspension at 60°C for 12 h. The suspension was then $Na^+$ exchanged with NaCl (1 mol $L^{-1}$) at pH = 7 for further dispersion (Lagaly, 2006). The salt surplus was eliminated through several phases of ultrapure water rinsing until the conductivity of the Na-suspension was lower than 5 μS $cm^{-1}$. The suspension was then left to sediment of 20.5 h at 20°C in accordance with Stokes law, and the size fraction smaller than 2 μm was recovered from the uppermost 20 cm of the suspension. The obtained Na-suspension was then freeze-dried and stored for further testing. This fraction contained 3.18% of organic C and exhibited a bulk cation-exchange capacity (CEC) level of 41.1 $cmol^+$ $kg^{-1}$ and an average single platelet size of 0.114 ± 0.1 μm as measured by transmission electron microscopy.

Sodium and Ca-suspensions were used in this study. The Na-suspensions were prepared through the simple redispersion of original Na-material in ultrapure water, followed by 12 h of agitation and 20 min of sonication at 47 kHz and 35 W. The Ca-suspensions were prepared by exchanging the Na-suspension with $10^{-1}$ M $CaCl_2$ under agitation conditions for 24 h and through the elimination of salt surplus as previously described. Both Na- and Ca-suspensions were prepared at 300 mg $L^{-1}$, a relevant solid content regarding soil solution (Cornu et al., 2014), and were used within 10 d.

### Characterization of *Lutum* Suspensions at a Stationary State

The Na- and Ca-suspensions were set under different pH or Ca concentration conditions through either the addition of NaOH or HCl solutions at $10^{-1}$ or $10^{-2}$ mol $L^{-1}$ or by adding $CaCl_2$ solutions at $10^{-2}$ up to 1 mol $L^{-1}$. The suspensions were then stirred for at least 12 h to reach a stationary state.

## Critical Coagulation Concentration

The critical coagulation concentration (CCC) of the Na-suspension was assessed for 100 mL Na-suspensions with pH levels of 4.4, 5.9, and 6.6 (Table 1). The particle and aggregate sizes were measured under stirring conditions at 15-s intervals over the course of the experiment via laser diffraction (MasterSizer 3000, Malvern Instruments). Calcium chloride increments ranging between $10^{-5}$ and $10^{-3}$ mol $L^{-1}$ were added every 5 min. The CCC value was defined as the Ca concentration range at which the aggregate size jump occurred.

## Electrophoretic Mobility

The electrophoretic mobility of particles in the Ca- and Na-suspensions was measured as a function of pH and Ca concentrations (Table 1) via laser Doppler velocimetry light scattering (ZetaSizer Nano ZS, Malvern Instruments). Triplicate measurements were performed.

## X-ray Diffraction

Tactoids that formed in Ca-suspensions under different Ca concentrations (Table 1) were analyzed by X-ray diffraction (XRD, PANanalytical X'PERT PRO X-ray apparatus with Co radiation) to determine the relative stacking of clay sheets. The analyzed suspensions were centrifuged at 48,400 *g* for 20 min. The pellets obtained were homogenized by mechanical shaking and then thinly spread over cleaned silicon, zero-background plates. After overnight drying under ambient atmosphere conditions, the orientated preparations were analyzed via XRD within a scanning range of $3° < 2\theta < 12°$ and over a counting time of 16.5 s per step at steps of 0.05°2θ.

## Cryogenic Scanning Electron Microscopy

The structural arrangement of the aggregated particles was assessed by cryogenic scanning electron microscopy (SEM XL series Philips XL 30S FEG apparatus). Calcium-suspensions equilibrated at different Ca concentrations ($6 \times 10^{-4}$ and $6 \times 10^{-5}$ mol $L^{-1}$) and pH levels (4 and 8) (Table 1) were left to sediment and were then analyzed. Sediment drops were placed on an Al holder and then instantly frozen in pasty N (−210°C) (Brisset, 2012). Before imaging, drops were held in the cryogenic stage at −90°C under high-vacuum conditions for approximately 1 h and 30 min to allow ice to sublimate and reveal particle arrangements.

## Aggregation and Dispersion Induced by pH or Calcium Concentration Modifications

To assess the impact of abrupt pH modifications or Ca concentration decline on Luvisol *lutum* aggregation or dispersion kinetics, batch experiments were conducted on the Ca-suspension. The experiments were carried in a 100-mL closed reactor, which was thermoregulated at 25 ± 0.5°C under N flux and gentle magnetic stirring conditions. A standard pH electrode was added to the reactor. The reactor was connected to the measuring cell of the Malvern laser particle sizer (Mastersizer MS3000, Malvern Instruments) under the recycling mode and at a constant flow rate (44 mL $min^{-1}$). The volume weighted particle-size distribution and pH levels were recorded at 10-s intervals over the course of the experiment. To express the time evolution of particle-size distribution, the cumulative percentage of particles smaller than 2 μm, hereafter called $\%P < 2$ μm, and Dv50 median size were used as indicators. To access structural information in the clay aggregates, the scattered intensity ($I$) as a function of the wave vector ($q$) was also studied (Guan et al., 1998; Lambert et al., 2000; Thill et al., 2001) based on a selection of representative measurements.

## pH Changes at Given Calcium Concentrations

The experiments were performed under three initial conditions: 100 mL of Ca-suspension at 300 mg $L^{-1}$ with a natural pH value of 5.9 were adjusted to Ca concentrations of $1.3 \times 10^{-5}$, $3.2 \times 10^{-4}$, and $1 \times 10^{-3}$ mol $L^{-1}$ (Table 1), which are hereafter, respectively referred to as $10^{-5}$, $10^{-4}$, and $10^{-3}$ $Ca^{2+}$. These concentrations were chosen based on their representativeness of concentrations encountered in rain ($10^{-5}$–$10^{-4}$ mol $L^{-1}$) (Chorover et al., 1994; Sanusi et al., 1996; Négrel and Roy, 1998; Ranger et al., 2001, 2007; Bertrand et al., 2008; Ladouche et al., 2009) and

**Table 1. Main physicochemical experimental conditions.**

| Experiment | Solid | | Electrolyte | |
|---|---|---|---|---|
| | Material | Solid concentration in suspension | $Ca^{2+}$ concentration | pH |
| | | mg $L^{-1}$ | mol $L^{-1}$ | pH unit |
| Zeta potential | Ca-particles | 300 | 0 to $10^{-2}$ | 3 to 8.5 |
| | Na-particles | 300 | 0 | 5.9 ± 0.3 |
| XRD | Na-particles | ND | 0 to $10^{-2}$ | 5.9 ± 0.3 |
| CCC† | Na-particles | 100 | 0 up to the CCC | 4.4 |
| | | | | 5.9 ± 0.3 |
| | | | | 6.6 |
| SEM‡ | Ca-particles | 300 | $5.9 \times 10^{-5}$ | 8 |
| | | | $6.2 \times 10^{-4}$ | 4 |
| TEM | Na-particles | 300 | less than $10^{-6}$ | 5.9 ± 0.3 |
| pH modification with constant $Ca^{2+}$ | Ca-particles | 300 | $10^{-5}$ $Ca^{2+}$: 1.3 ± 0.2 x $10^{-5}$ | 4.5, 5.1, 7.9 |
| | | | $10^{-4}$ $Ca^{2+}$: 3.2 ± 0.5 x $10^{-4}$ | 4.1, 5, 7.3 |
| | | | $10^{-3}$ $Ca^{2+}$: 1.1 ± 0.14 x $10^{-3}$ | 4.3, 5, 7.1, and 7.5 |
| $Ca^{2+}$ modification with constant pH | Ca-particles | 300 | $6.2 \times 10^{-5}$ | 4.3 |
| | | | | 5 |
| | | | | 6.4 |
| | | | | 7.6 |

† CCC, critical coagulation concentration.
‡ SEM, scanning electron microscopy.

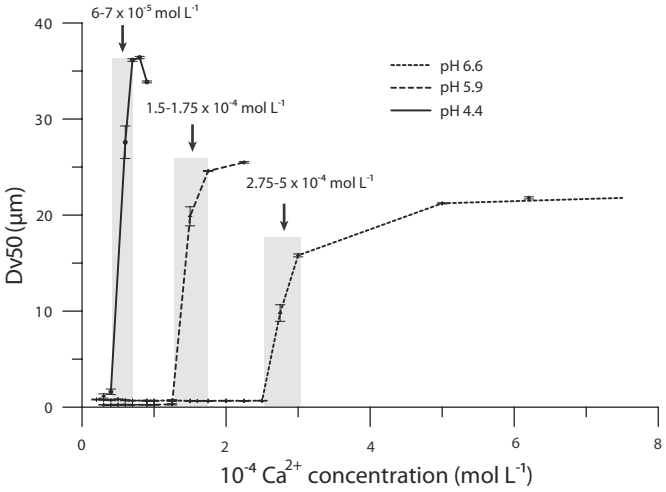


**Fig. 1. Dv50 as a function of Ca concentration. The Dv50 value was recorded 5 min after each Ca increment. Gray rectangles represent the critical coagulation concentration range.**

in lysimeter-sample soil water ($10^{-5}$–$10^{-3}$ mol $L^{-1}$) (Howitt and Pawluk, 1985; Swistock et al., 1990; Johnson, 1995; Marques et al., 1996; Gallet and Keller, 1999; Ranger et al., 2001; Citeau et al., 2003; Ranger et al., 1993; Vrbek, 2005; Ranger et al., 2007; Löhr and Cox, 2012; Watmough et al., 2013; SOERE ACBB, unpublished data, 2014). At $t_0$, the pH was quickly adjusted from 5.9 to approximately 4, 5, 7, or 8 (typical pH values in soils) through the addition of either NaOH or HCl.

## Calcium Concentration Dilution at Given pH Levels

In this experiment, 10 mL of 3 g $L^{-1}$ Ca-suspension were prepared in 6.2 × $10^{-4}$ mol $L^{-1}$ $CaCl_2$ at pH levels ranging from 4 to 8 (Table 1) and then left to equilibrate overnight. At $t_0$, these suspensions were diluted 10 times by adding 90 mL of ultrapure water that had been previously adjusted to the corresponding pH values. This dilution ratio mimics soil water dilution characteristics caused by rainwater events.

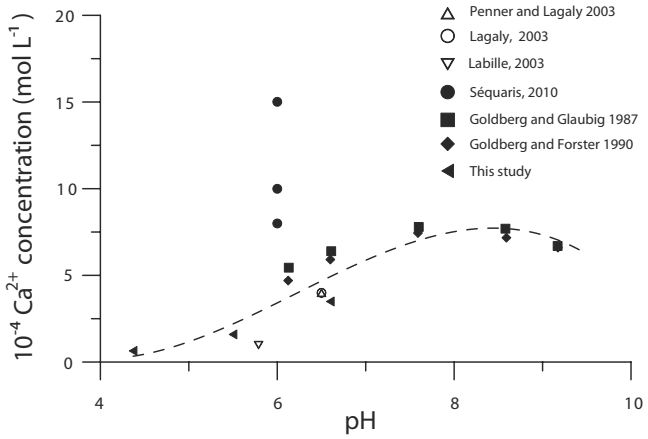


**Fig. 2. Critical coagulation concentration as a function of pH for a $CaCl_2$ electrolyte and solid concentration lower than 0.7 g $L^{-1}$. Open shapes denote model clays and filled shapes denote soil clays. The dotted line represents a model fit.**

# RESULTS

## Characterizations of Suspensions at the Stationary State

### Critical Coagulation Concentration

Increasing the Ca concentration of the solution resulted in clay aggregation in the suspension once the CCC was reached. When the pH level decreased from 6.6 to 4.4, the CCC decreased from 2 to 5 × $10^{-4}$ to 6 to 7 × $10^{-5}$ mol $L^{-1}$, and the aggregate size above the CCC threshold increased from approximately 20 to 35 µm (Fig. 1). These CCC values were compared to data from literature that examined either model (Penner and Lagaly, 2000; Labille, 2003; Lagaly and Ziesmer, 2003) or soil smectite (Goldberg and Glaubig, 1987; Goldberg and Forster, 1990; Séquaris, 2010) and which studied low clay concentrations (<0.7 g $L^{-1}$), as Labille (2003) and Penner and Lagaly (2000) demonstrated that the CCC values increase with solid concentration. No data on pH levels less than 5 were found in the literature (Fig. 2). With the exception of the work by Séquaris (2010), the CCC values follow a growing trend of increasing pH for all materials considered. No clear distinction was found between model and soil smectite in relation to their respective CCC values in the pH domain considered.

## Electrophoretic Mobility

The electrophoretic mobility of the Ca-suspensions at soil pH (5.9 ± 0.3) first increased abruptly from −2.17 to −0.92 × $10^{-8}$ $m^2$ $s^{-2}$ $V^{-1}$ while the electrolyte Ca concentration increased from 0 to 5 × $10^{-4}$ mol $L^{-1}$, crossing the CCC, and then increased moderately up to −0.5 × $10^{-8}$ $m^2$ $s^{-2}$ $V^{-1}$ at 5 × $10^{-3}$ mol $L^{-1}$ (Fig. 3). The same trend was observed by Labille (2003) for model smectite and by Grolimund et al. (2001) and Séquaris (2010) for soil clays (Fig. 3), though a slightly higher degree of electrophoretic mobility was measured at the plateau for the present clay. Again, only slight differences were observed between soil and model smectites.

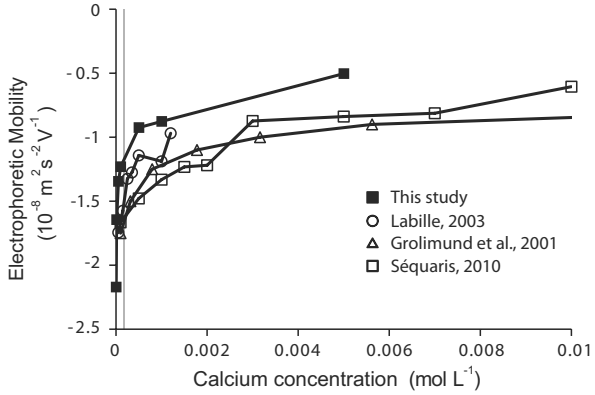


**Fig. 3. Electrophoretic mobility of Ca-smectite suspensions at a stationary state as a function of Ca concentration. Filled shapes denote data obtained through this study for a suspension at soil-pH (5.9 ± 0.3). The critical coagulation concentration measured at the same pH level is denoted by the gray line. Open shapes denote literature data for model or soil smectite at 5.7 < pH < 6 (Circle: Labille, 2003 for model montmorillonite; triangle: Grolimund et al., 2001 for soil particles; square: Séquaris, 2010 for soil particles).**

The electrophoretic mobility of the clay particles in the Na-suspension increased significantly when the pH level dropped from 6 to 3, and no measurable effect was observed when the pH level increased (Fig. 4). This trend was less significant for Ca-suspensions, as the electrophoretic mobility value already ranged between more neutral values from −2 to −0.1 $m^2 s^{-2} V^{-1}$. A slight increase in the value of electrophoretic mobility was observed when the $CaCl_2$ concentration increased from $5 \times 10^{-6}$ to $10^{-2}$ mol $L^{-1}$. Meanwhile, the global charge of the Ca-clay particles remained negative over the whole range of $Ca^{2+}$ concentrations and pH levels tested. This confirms that (i) the divalent cation sorption level at the clay surface partially neutralizes the permanent negative structural charge expressed at the basal plane (Avena and De Pauli, 1998; Lagaly, 2006; Tournassat et al., 2011) and (ii) that amphoteric edges compose a small proportion of the clay in terms of the surface (1%) (Sondi et al., 1997) and total charge (5–27%) (Anderson and Sposito, 1991; Wanner et al., 1994; Tournassat et al., 2003; Lagaly, 2006) of the dominant negative structural charge. The small collection of available studies that examined comparable experimental conditions (Chorom and Rengasamy, 1995; Kjaergaard et al., 2004) provide comparable electrophoretic mobility values and evolution trends (Fig. 4) regardless of whether the clay origin studied was either hydrothermal or pedogenetic.

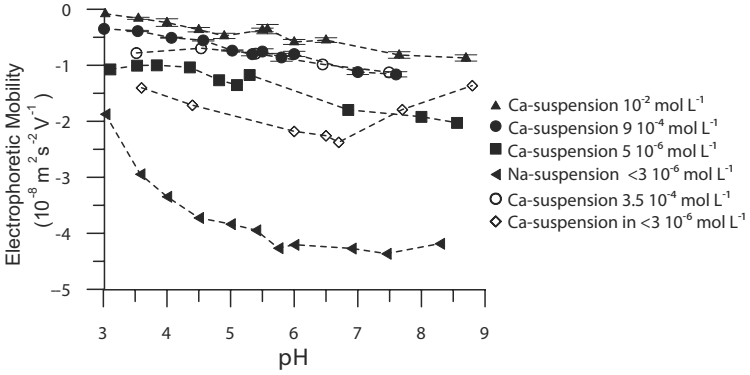


**Fig. 4. Electrophoretic mobility of suspensions as a function of pH, electrolyte background, and clay interlayer space cation. Filled shapes denote data from this study, while open shapes denote data from the literature (circle: soil Ca-smectite in 3.5 × $10^{-4}$ mol $L^{-1}$ $CaCl_2$ by Kjaergaard et al., 2004; square: model Ca-smectite in distilled water by Chorom and Rengasamy, 1995).**

## State of Aggregation at the Stationary State

The state of aggregation of the suspension was measured at a stationary state, that is, after 12 h of equilibration, for different Ca concentrations and pH levels. As expected, the Dv50 increased abruptly, passing the CCC value and reaching 6- to 7-fold higher at $10^{-4}$ (10 μm) than at $10^{-5}$ mol $L^{-1}$ $Ca^{2+}$ (1.5 μm) (Fig. 5a). As the salt concentration continued to increase, the Dv50 finally leveled at approximately 12 μm. The opposite trend was observed for %*P* < 2 μm (Fig. 5a) but with no difference found between the two highest Ca concentrations. In addition, the particle-size distributions obtained for the three Ca concentrations exhibited a bimodal distribution (Fig. 5b). At $10^{-5}$ $Ca^{2+}$, the first mode was centered on 0.7 μm and the second centered on 3 μm, with both populations exhibiting approximately the same volume proportion. At higher Ca concentrations, the 0.7 μm population remained only to a minor extent, while the larger population had grown both in proportion and size, centering on 10 μm and 15 μm at $10^{-4}$ $Ca^{2+}$ and $10^{-3}$ $Ca^{2+}$, respectively. Such an evolution with salt concentrations is characteristic of aggregation mechanisms induced by salt, which incorporates the smallest particles into larger aggregates.

## X-Ray Diffraction Patterns

The XRD-patterns obtained for the particles of Na-suspensions equilibrated with Ca at different concentrations showed a change in smectite peak levels from approximately 12.5 to 14.5 Å under increasing Ca concentration conditions (Fig. 6). This was related to cation exchange in the interlayer space from a single water layer smectite (standard *d001* peak at 12.3–12.8 Å) to a double water layer smectite (standard *d001* peak at 14.8–15.8 Å) (Hubert, 2008), which correspond with the effective exchange of $Na^+$ and $Ca^{2+}$, respectively. From the deconvolution of this smectite diffraction peak (Fityk-software; Wojdyr, 2010), we estimated the relative proportion of Ca-exchanged smectite for the different Ca concentrations. This proportion increased logarithmically with the Ca concentration (Fig. 7). In addition, the *d001* peak for the Ca-exchanged smectite appeared to be considerably better defined than that of the original Na-smectite. This signifies a longer coherent domain in the basal plane in the former case.

## Structural Arrangement of Clay Particles

The structural arrangement of clay particles at the micrometric scale obtained at pH 8, $[Ca^{2+}] = 5.9 \times 10^{-5}$ mol $L^{-1}$, and

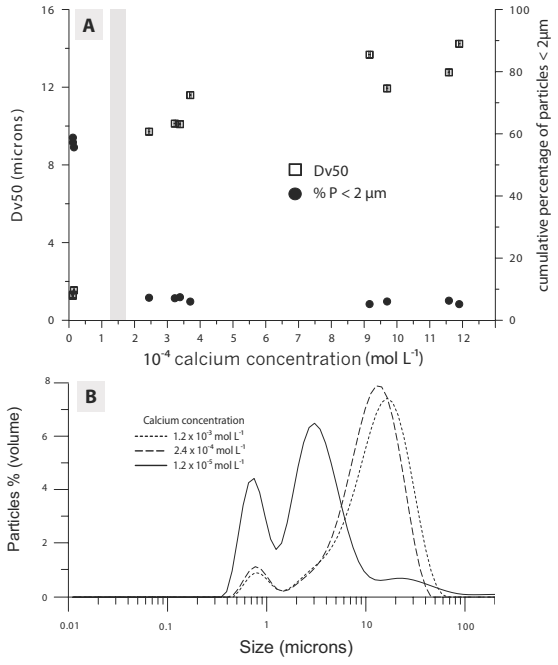


**Fig. 5. Aggregate and particle size distribution of suspensions at a stationary state at pH 5.9 ± 0.3: (a) Dv50 and %*P* < 2 μm as a function of Ca concentration. The critical coagulation concentration at the same pH value is reported as a gray rectangle. (b) Particle size distribution for three Ca concentrations.**

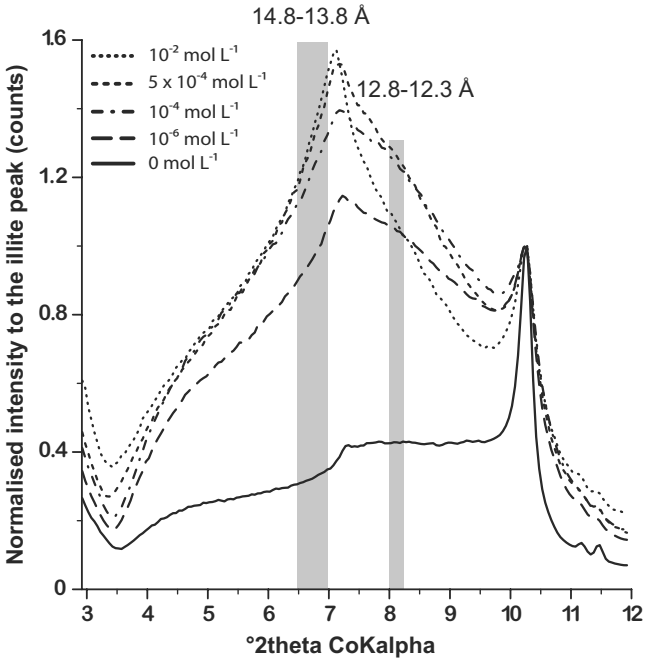


**Fig. 6. X-ray diffraction-pattern obtained for Na-suspensions equilibrated with different Ca-electrolyte concentrations. X-ray diffraction patterns were normalized to the illite peak. Gray rectangles represent the d range for Na-smectite and Ca-smectites drawn from the literature.**

pH 4, $[Ca^{2+}] = 6.2 \times 10^{-4}$ mol $L^{-1}$, respectively, are presented in the cryo-SEM micrographs shown in Fig. 8. In both cases, clay deposits exhibit comparable structures in which compact submicrometric units are connected, forming a loose and three-dimension network at the larger scale (Fig. 8). No significant distinction could be made at this scale of observation with respect to pH and Ca levels.

## Aggregation and Dispersion Kinetics Induced by pH and/or Calcium Modification

### Change in pH at a Given Calcium Concentration

For all of the initial Ca concentrations considered, base additions increased %$P$ < 2 μm levels and decreased Dv50 levels,

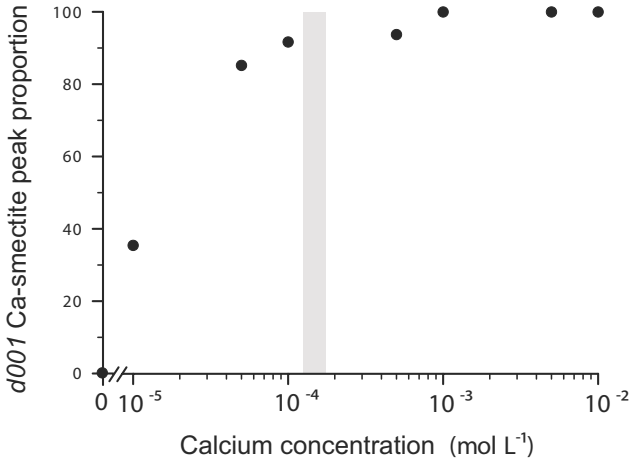


**Fig. 7. Relative intensity of the *d001* Ca-smectite peak as a function of Ca concentration. The critical coagulation concentration at soil-pH (5.9 ± 0.3) is reported as a gray rectangle.**

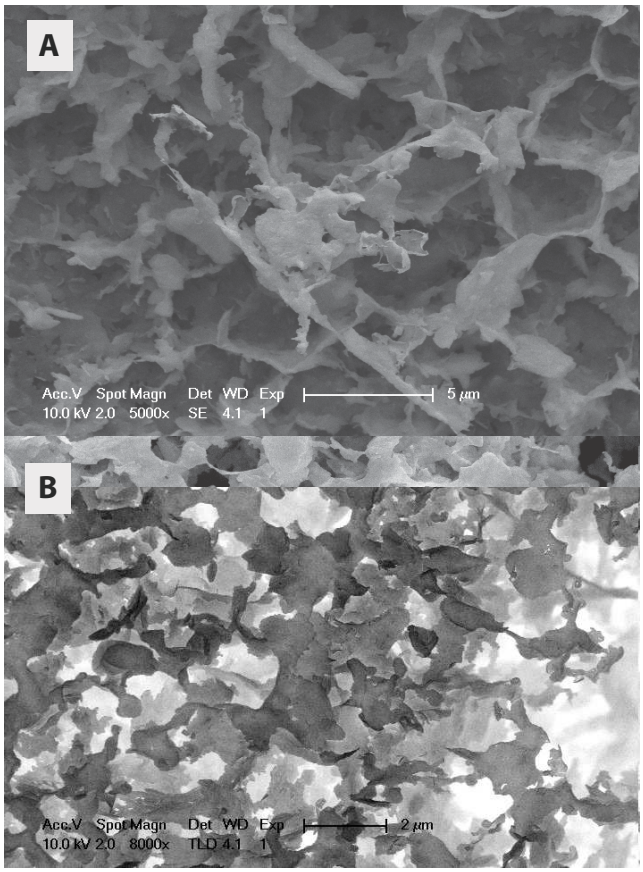


**Fig. 8. Scanning electron microscopy photographs of the Ca-suspension observed at the cryogenic stage: (a) pH 8 and $[Ca^{2+}] = 5.9 \times 10^{-5}$ mol $L^{-1}$ and (b) pH 4 and $[Ca^{2+}] = 6.2 \times 10^{-4}$ mol $L^{-1}$.**

and the opposite trends were observed for acidification (Fig. 9). However, the amplitude of size modifications caused by pH perturbations was found to be a function of the initial Ca concentration. The acidic-induced aggregation was especially marked at the lowest $Ca^{2+}$ concentration ($10^{-5}$ mol $L^{-1}$), while the basic-induced dispersion was clearer at $10^{-4}$ $Ca^{2+}$. At the highest $Ca^{2+}$ concentration ($10^{-3}$ mol $L^{-1}$), acidic and basic perturbations were "inhibited" by high initial Ca concentrations with the exception of further aggregation trend observed at the 4.3 pH level.

Aggregation and dispersion kinetic processes generally followed two successive phases: (i) a high aggregation or dispersion rate within the first minutes followed by (ii) a partial reversal toward a steady state plateau in the case of prior aggregation or toward a direct plateau in the case of dispersion (Fig. 9). Indeed, the rapid aggregation trend achieved in the first phase resulted in the formation of unstable aggregates with regards to shearing forces, which were subsequently broken in reaching a steady state. This transitory phenomenon was observed by Labille et al. (2003) in relation to the rapid aggregation of clay by polysaccharides. The final aggregation states obtained after 1 h of monitoring were compared to the values obtained at the stationary state with $6 \times 10^{-4}$ mol $L^{-1}$ $Ca^{2+}$ (Fig. 10). At pH = 4, the stationary state was comparable to the 1 h states for both $10^{-3}$ and $10^{-4}$ $Ca^{2+}$, while at pH = 7.5, the stationary state was only comparable to the 1 h state for $10^{-4}$ M $Ca^{2+}$. This suggests that under

these conditions, due to a favoring of aggregation or dispersion, respectively, the stationary state will be reached within 1 h. However, under more balanced conditions, that is, pH 5 to 7, aggregates remaining after 1 h are larger than those obtained after the 12-h equilibration period.

## Dilution of the $Ca^{2+}$ Concentration at a Given pH

The abrupt decrease in Ca concentration from $6.2 \times 10^{-4}$ to $6.2 \times 10^{-5}$ mol $L^{-1}$ with the dilution of concentrated *lutum* suspensions with pure water content adjusted at targeted pH levels (Table 1) did not induce a significant change in the Dv50 level for the four pH values tested (Fig. 11). The slight variations observed during the first minutes of the test are attributable to rapid pH equilibration between the diluting solution and the concentrated *lutum* suspension; the pH of this latter material after overnight equilibration deviated slightly. The evolution of %$P$ < 2 μm was also nearly negligible except at a pH level of 8, during which an increase from 40% to more than 60% was recorded after 6 h.

## Structural Arrangement of Clay Particles Analyzed by Static Light Scattering

In the log/log plot of the scattered intensity as a function of the wave vector (Fig. 12), an inflection point is observed at $q = 5.17$ μm$^{-1}$. This implies the coexistence of two distinct structures both below and above the corresponding scale of 0.6 μm. We attribute this characteristic size to that of elementary tactoids, as it coincides well with the initial fractionation of particles smaller than 2 μm. At larger $q$ values ($5.17 < q < 9.47$ μm$^{-1}$), Ca-particles were more compact and characterized by an $I(q)$ slope of 2.7, while the slope was found to be 2.3 for Na-particles. At smaller $q$ values (Guinier plateau < $q$ < 5.17 μm$^{-1}$), a long, linear domain was present for Ca-particles, denoting a fractal structure. The slope of this domain (i.e., the fractal dimension) was 2.1 ± 0.15 and exhibited no evident variation regardless of the Ca concentration or pH level considered. The inflection to the Guinier plateau observed at smaller wave vectors characterizes the maximum aggregate size and is in good agreement with the laser diffraction interpretations presented in Fig. 9.

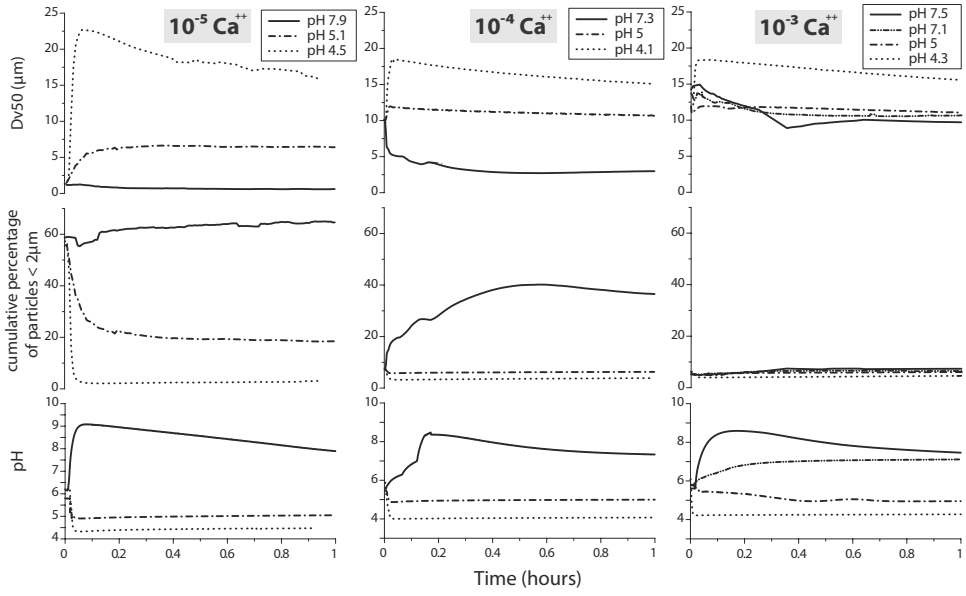


**Fig. 9. Dv50, %$P$ < 2 μm and pH evolution as a function of time for the three Ca concentrations. pH perturbations were applied at a time equal to zero.**

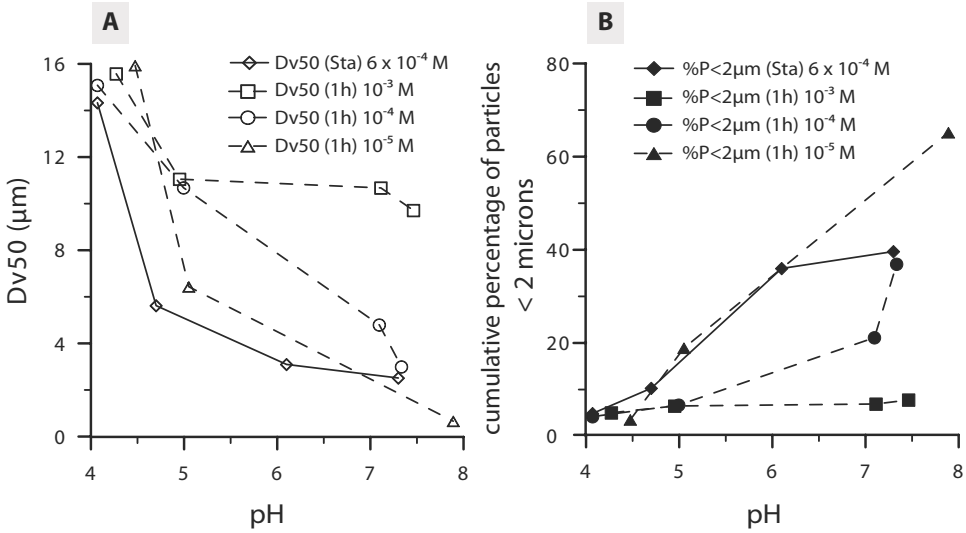


**Fig. 10. Dv50 and %$P$ < 2 μm of the Ca-suspensions as a function of pH and $CaCl_2$ background at stationary state (Sta) and an hour (1 h) after pH perturbation.**

# DISCUSSION

## Phase Diagram as a Function of Calcium and pH

Effects of pH and Ca concentration on clay particles stability remain difficult to dissociate among the various colloidal dynamics of clay particles, even when their respective actions can be clearly distinguished from a conceptual point of view. It is widely assumed, based on works examining model smectite, that pH controls interactions due to the protonation of clay edges while Ca as interlayer counterion shapes interactions between clay faces. Our experiments show that both Ca concentrations and pH levels have an interrelated effect on soil *lutum* dispersion and aggregation.

In combining the literature data with our experimental results, we proposed the following phase diagram for Luvisol *lutum* as a function of pH and Ca concentrations (Fig. 13a). This diagram aims to more effectively specify the effects of the two pa-

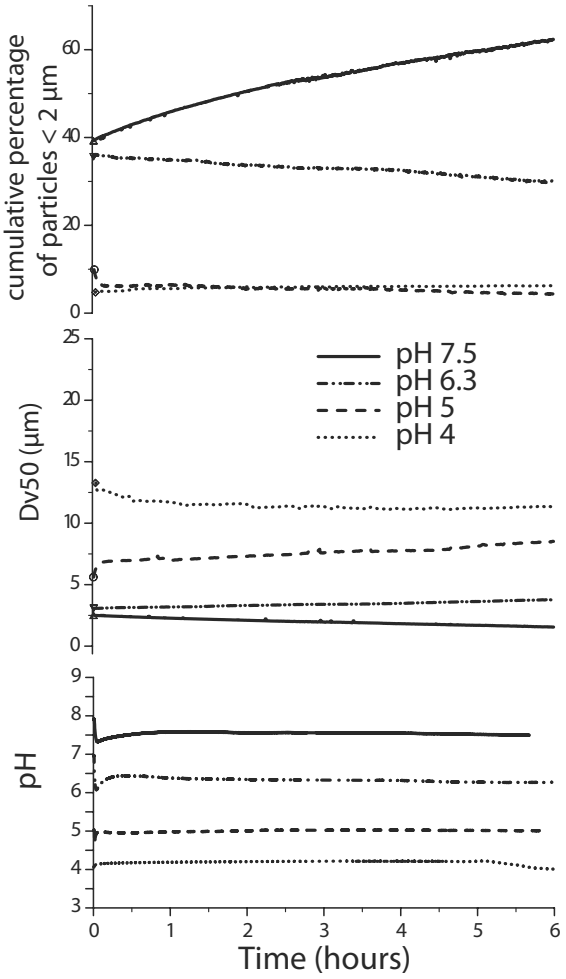


**Fig. 11. Dv50 and %*P* < 2 µm evolution after suspension dilution at the stationary state and under three different initial pH levels.**

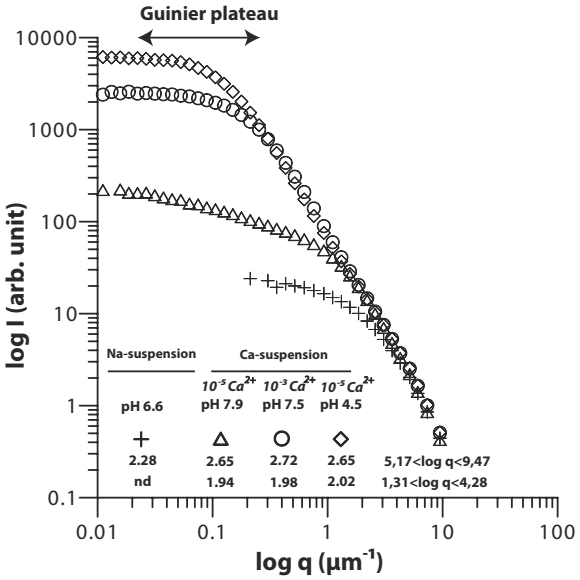


**Fig. 12. Scattered intensity (*I*) as a function of the wave vector (*q*) for Na- and Ca-suspensions at different Ca concentrations and 1 h after pH perturbation. The slope of the linear portion of the (log *I*) vs. (log *q*) plot is correlated with aggregate compactness (fractal domain).**

rameters on the expected behavior of clay particles under conditions relevant to soil pore water. The pH level of edge zero-charge ($pH_{PZC\ edge}$) is a crucial characteristic as it determines the extent of protonation in clay edges as a function of pH. The median value ($pH_{PZC\ edge}$ = 6.5) and third quartile were calculated from literature results for approximately 2:1 clay minerals and are reported in Fig. 13 (Heath and Tadros, 1983; Brandenburg and Lagaly, 1988; Lagaly, 1989; Permien and Lagaly, 1994; Avena and De Pauli, 1998; Benna et al., 1999; Wanner et al., 1994; Keren and Sparks, 1995; Manning and Goldberg, 1996; Thomas et al., 1999; Durán et al., 2000; Tombacz and Szekeres, 2004; Delhorme et al., 2010). The clay aggregate formation is thus balanced according to both the CCC and $pH_{PZC\ edge}$ thresholds.

For all of the tested Ca concentrations, at pH levels of 5 and 4, particles exist in an aggregated state as shown in Fig. 9 and 10. This is in agreement with results from the literature (Van Olphen, 1977; Hesterberg and Page, 1990; Gu and Doner, 1992; Durán et al., 2000) and shows that at pH < $pH_{PZC\ edge}$, edges protonation enhances the electrostatic attraction between clay platelets and produces an aggregated state irrespective of the Ca concentration tested.

At pH levels higher than seven, which are most likely higher than the $pH_{PZC\ edge}$, the aggregation state depends on the Ca concentration background (Fig. 10). Increasing the Ca concentration led to an abrupt increase in electrophoretic mobility (Fig. 3), suggesting that decreased electrostatic repulsions are the driving force behind particle aggregation above the CCC.

Moreover, the aggregation was certainly enhanced by the divalent properties of interlayer counterion $Ca^{2+}$, which favors face–face clay sheet stacking (Hunter, 1981; Kinsela et al., 2010; Kjaergaard et al., 2004; Lagaly, 2006; Séquaris, 2010). The presence of this arrangement is confirmed by the stronger definition of the *d001* Ca-smectite diffraction peak (Fig. 6 and 7) compared to the Na-smectite and by the more compact structure of Ca-tactoids revealed by static light scattering (Fig. 12).

At scales larger than the tactoid, static light scattering and cryo-SEM levels (Fig. 8) indicate a fractal and looser aggregate structure that assembles dense elementary tactoids. This suggests that aggregates are composed of 0.6-µm tactoids and that the internal structure of the latter was not significantly modified by subsequent aggregation dynamics induced by the change in solution chemistry. No evident structural distinction could be made at these two scales between aggregates induced by acid pH and aggregates induced by Ca.

## Aggregation State Dynamics and Reversibility

Calcium and pH concentrations may have cumulative and competing effects on the dispersion vs. aggregation tendencies of the *lutum* suspension. The balance of these effects heavily drives the kinetics and potential reversibility of mechanisms involved. The aggregation kinetics at Ca concentrations of >CCC or pH levels of <5 were quite rapid (i.e., 10 min) (Fig. 1 and 9) and reflect so-called processes of fast coagulation (Missana and Adell, 2000; Kjaergaard et al., 2004; Furukawa et al., 2009; Séquaris,

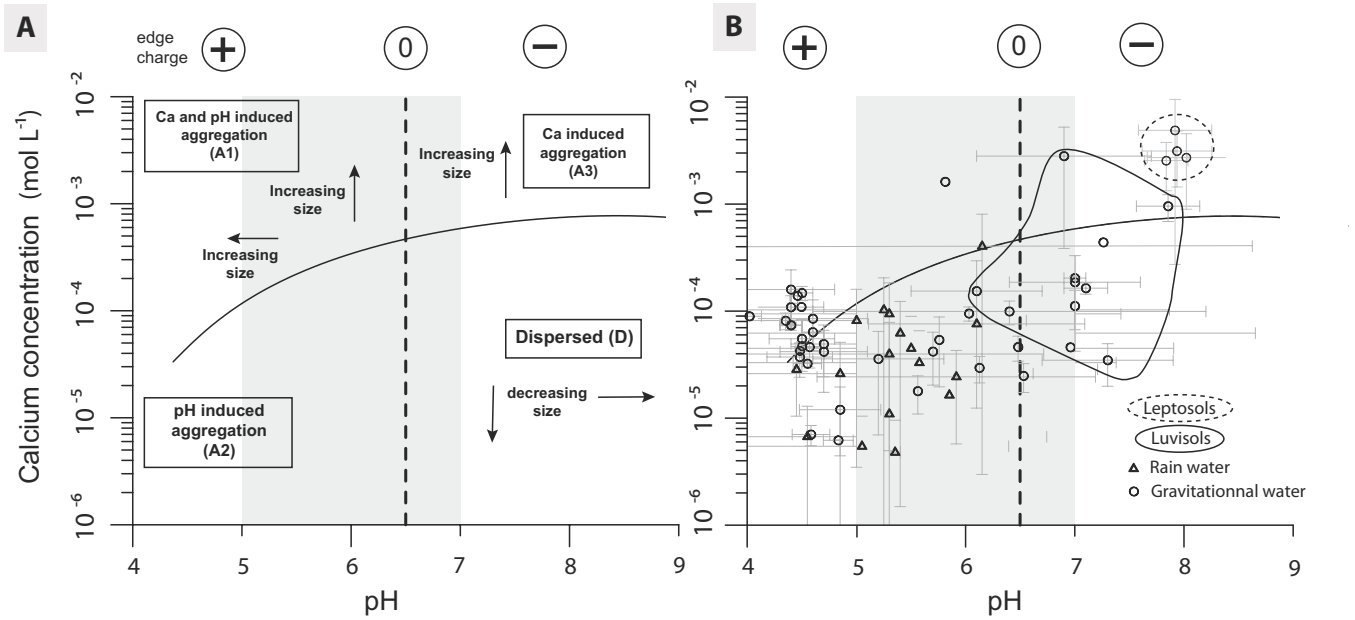


**Fig. 13. Phase diagram for Ca-suspension as a function of pH and Ca concentration. The solid line represents the critical coagulation concentration (CCC) as a function of pH. The dotted line represents the median value of the pH $_{PZC\ edges}$, and the gray rectangle represents the first and third quartiles of the pH $_{PZC\ edges}$. (a) Particle association type as a function of pH and Ca concentration. (b) Rainwater and gravitational water chemistry values drawn from the literature.**

2010). Such a time scale is compatible with the persistence time of gravitational water in soil.

The aggregate redispersion induced by increasing pH in $10^{-4}$ $Ca^{2+}$ suspensions was achieved within a similar time scale (Fig. 9), indicating relatively good reversibility in the aggregation state obtained under this condition. Indeed, under such intermediate Ca concentrations, the pH change shifts the system to below the CCC ($CCC_{pH\ 6.6} = 2.75 - 5 \times 10^{-4}$ mol $L^{-1}$ $CaCl_2$, Fig. 1), which allows the aggregates to redisperse. However, reversibility was not observed systematically. Whereas the drastic decrease in Ca concentrations from $6.2 \times 10^{-4}$ to $6.2 \times 10^{-5}$ mol $L^{-1}$ induced redispersion only at the highest level of pH (7.5) tested (Fig. 10), final Ca concentrations fell below the CCC threshold at pH levels of 5 and 6 as well (Fig. 1). The non-redispersion of clay aggregates at these two latter pH levels despite the occurrence of diffuse double layer expansion suggests partial irreversibility in the aggregation induced by Ca, at least with respect to the 6-h time scale of this experiment. This is attributable to the high affinity of Ca cation on the clay surface and the shared position of two neighbor faces. Both of these characteristics likely limit divalent cation mobility (Tournassat et al., 2003). Only the most basic condition tested (pH 7.5) was able to balance and overcome attractive interparticle forces induced by Ca. Finally, at the highest Ca concentration tested, $10^{-3}$ $Ca^{2+}$ (Fig. 9), the pH effect became minor and negligible with respect to that of the aggregating Ca. Only the most acidic pH perturbation (i.e., pH 4.3) induced even further aggregation due to the presence of increased interparticle attraction. For all of the higher pH conditions tested, the system remained "buffered" and aggregated by high Ca concentrations.

## Implications for Particle Migration in Soils

In relating these results to soil solution chemistry and deducing their potential implications for the physical chemistry of particle migration in soil pores, we compiled Ca concentrations and pH values of soil water sampled by lysimeters provided in the existing literature (Howitt and Pawluk, 1985; Swistock et al., 1990; Johnson, 1995; Marques et al., 1996; Gallet and Keller, 1999; Ranger et al., 2001; Citeau et al., 2003; Ranger et al., 1993; Vrbek, 2005; Ranger et al., 2007; Löhr and Cox, 2012; Watmough et al., 2013; SOERE ACBB, unpublished data, 2014). Rainwater monitoring values were also gathered (Fig. 13b) (Chorover et al., 1994; Sanusi et al., 1996; Négrel and Roy, 1998; Ranger et al., 2001, 2007; Bertrand et al., 2008; Ladouche et al., 2009; SOERE ACBB, unpublished data, 2014). These pH and Ca concentration data are drawn from California (Chorover et al., 1994) and from various sites throughout France (Bertrand et al., 2008; Ladouche et al., 2009; Négrel and Roy, 1998; Ranger et al., 2007, 2001; Sanusi et al., 1996; SOERE ACBB unpublished data, 2014). The pH values range from 4.8 to 6.1, while Ca concentrations range from $10^{-6}$ to $10^{-4}$ mol $L^{-1}$, with seasonal variability values typically being higher than spatial variability levels.

While rainwater appears to be too acidic to disperse aggregated soil particles based on physicochemical reactions as shown in Fig. 13b, it may mobilize particles via physical mechanisms (splash effect, shear force, etc.).

Water sampled from lysimeters exhibited a greater range of pH than rainwater, illustrating soil type chemistry variations. Luvisol gravitational water is globally located in the dispersed section of the phase diagram (Fig. 13b). Preexisting aggregates must therefore be fragile, likely undergoing mobilization within percolating water. In acidic soils (pH < 5), the composition of

gravitational soil water is positioned in the aggregated section of the diagram due to protonated clay sheet edges, suggesting the development of a *lutum* that is initially heavily aggregated. According to our data (Fig. 9) and literature (Fig. 13b), aggregate dispersion through an increase of pH to higher than 7, is not likely to occur because rainwater pH is too acidic in most cases. This pH threshold is in agreement with those classically defined in the literature on eluviation (Quénard et al., 2011). However, regarding Leptosols (pH > 7.5), which is also located in the aggregating condition of the diagram but due to high Ca concentrations, our results suggest that salt dilution induced by rainfall events is not fast enough (<1 h) to reverse preexisting aggregates synchronously with gravitational water infiltration.

The dispersed *lutum*, which may potentially migrate to deeper soil horizons through the soil pore network, may aggregate and deposit according to variations in soil solution chemistry. For Luvisols, according to Fig. 13b, particles will remain dispersed in most cases. This suggests that illuviation is not likely to occur within macropores for physicochemical reasons but may rather be caused by physical filtration in the surrounding matrix of lower porosity. In the case of acidic soils and Leptosols, previously dispersed and migrating *lutum* is expected to undergo aggregation to a size of a few tens of micrometers (Fig. 9). The aggregates may then be trapped or excluded by smaller pores. The released material may consequently only migrate through macropores larger than a few tens of micrometers, which represent only a small proportion of the total porosity and which thus exhibit limited degrees of mobility in most cases.

## CONCLUSION

This work aimed at investigating the role of physicochemical interactions that occur during clay particle mobility processes in soils. We studied the colloidal dynamics of clay particles (*lutum*) extracted from a luvisol and compared these to dynamics of pure and crystalline clay minerals. We focused on realistic soil physicochemical conditions (pH, Ca concentration) and on time scales that correspond with gravitational water infiltration processes. We conclude that:

1. The conditions for dispersion stability among the *lutum* particles are similar to those known for model smectites.

2. The kinetics of particle aggregation vs. dispersion in soil solution conditions are rapid enough to occur synchronously with soil macropore water transfer.

3. Aggregation and dispersion may thus take place within gravitational soil water depending on the nature of chemical perturbation induced by rainfall.

In terms of soil formation, we deduce from these results that physicochemical mechanisms may play a significant role in soil eluviation and illuviation. Suspended particle aggregation is likely to induce particle trapping or exclusion by smaller pores, which may inhibit eluviation and favor illuviation. Such mechanisms must, therefore, be explicitly implemented through soil formation models (Finke, 2012) or particle transport models (Jarvis et al., 1999).

While our methodological approach is relevant for particles that are already suspended in gravitational water, the physicochemical processes that drive particle release from the surrounding soil matrix to gravitational soil water must be investigated further. Higher solid/solution ratios may modify CCC thresholds. Additionally, while the quantity of natural organic matter was minimized in this work to better distinguish pH from counter-ion effects, this nevertheless plays a dominant role in soil structuration and aggregation. Finally, percolation column experiments should allow for more accurate distinction and weigh calculations of the contributions of physicochemical and physical mechanisms. To fully understand natural field process variability, further investigations should focus on the influence of other soil constituents such as organic matter, Fe oxides, and active pore network structural characterizations.

## ACKNOWLEDGMENTS

The authors are grateful to the French Research Agency ANR for funding the Agriped project (ANR 10 Blanc 605), to the French PACA Region and Parc des Baronnies provencales for the funding of a PhD grant, to Patrick Signoret for carbon analyses, and to the INRA AgroImpact unit for granting access to soil water chemistry data of SOERE ACBB for Mons en Chaussée and Lysimeter device of Fagnières. Cryo SEM observations were performed at the CP2 M of the University of Marseille.

## REFERENCES

Abend, S., and G. Lagaly. 2000. Sol–gel transitions of sodium montmorillonite dispersions. Appl. Clay Sci. 16:201–227. doi:10.1016/S0169-1317(99)00040-X

Amrhein, C., P.A. Mosher, and J.E. Strong. 1993. Colloid-assisted transport of trace metals in roadside soils receiving deicing salts. Soil Sci. Soc. Am. J. 57:1212–1217. doi:10.2136/sssaj1993.03615995005700050009x

Anderson, S.J., and G. Sposito. 1991. Cesium-adsorption method for measuring accessible structural surface charge. Soil Sci. Soc. Am. J. 55:1569–1576. doi:10.2136/sssaj1991.03615995005500060011x

Avena, M.J., and C.P. De Pauli. 1998. Proton adsorption and electrokinetics of an Argentinean montmorillonite. J. Colloid Interface Sci. 202:195–204. doi:10.1006/jcis.1998.5402

Benna, M., N. Kbir-Ariguib, A. Magnin, and F. Bergaya. 1999. Effect of pH on rheological properties of purified sodium bentonite suspensions. J. Colloid Interface Sci. 218:442–455. doi:10.1006/jcis.1999.6420

Bertrand, G., H. Celle-Jeanton, P. Laj, J. Rangognio, and G. Chazot. 2008. Rainfall chemistry: Long range transport versus below cloud scavenging. A two-year study at an inland station (Opme, France). J. Atmos. Chem. 60:253–271. doi:10.1007/s10874-009-9120-y

Bockheim, J.G., and A.N. Gennadiyev. 2000. The role of soil-forming processes in the definition of taxa in Soil Taxonomy and the World Soil Reference Base. Geoderma 95:53–72. doi:10.1016/S0016-7061(99)00083-X

Borgnino, L. 2013. Experimental determination of the colloidal stability of Fe(III)-montmorillonite: Effects of organic matter, ionic strength and pH conditions. Colloids Surf. A 423:178–187. doi:10.1016/j.colsurfa.2013.01.065

Brandenburg, U., and G. Lagaly. 1988. Rheological properties of sodium montmorillonite dispersions. Appl. Clay Sci. 3:263–279. doi:10.1016/0169-1317(88)90033-6

Brisset, F. 2012. Microscopie électronique à balayage et microanalyses. SOFEDIS, Paris.

Chorom, M., and P. Rengasamy. 1995. Dispersion and zeta potential of pure clays as related to net particle charge under varying pH, electrolyte concentration and cation type. Eur. J. Soil Sci. 46:657–665. doi:10.1111/j.1365-2389.1995.tb01362.x

Chorover, J., P.M. Vitousek, D.A. Everson, A.M. Esperanza, and D. Turner. 1994. Solution chemistry profiles of mixed-conifer forests before and after fire. Biogeochemistry 26:115–144. doi:10.1007/BF02182882

Citeau, L., I. Lamy, F. van Oort, and F. Elsass. 2003. Colloidal facilitated transfer of metals in soils under different land use. Colloids Surf. A 217:11–19. doi:10.1016/S0927-7757(02)00554-X

Cornu, S., L. Quénard, I. Cousin, and A. Samouëlian. 2014. Experimental approach of lessivage: Quantification and mechanisms. Geoderma 213:357–370. doi:10.1016/j.geoderma.2013.08.012

de Jonge, H., O.H. Jacobsen, L.W. de Jonge, and P. Moldrup. 1998. Colloid-facilitated transport of pesticide in undisturbed soil columns. Phys. Chem. Earth 23:187–191. doi:10.1016/S0079-1946(98)00011-1

de Jonge, L.W., C. Kjærgaard, and P. Moldrup. 2004. Colloids and colloid-facilitated transport of contaminants in soils. Vadose Zone J. 3:321–325. doi:10.2136/vzj2004.0321

Delhorme, M., C. Labbez, C. Caillet, and F. Thomas. 2010. Acid-base properties of 2:1 clays. I. Modeling the role of electrostatics. Langmuir 26:9240–9249. doi:10.1021/la100069g

Durán, J.D.G., M.M. Ramos-Tejada, F.J. Arroyo, and F. González-Caballero. 2000. Rheological and electrokinetic properties of sodium montmorillonite suspensions: I. Rheological properties and interparticle energy of interaction. J. Colloid Interface Sci. 229:107–117. doi:10.1006/jcis.2000.6956

Elsass, F. 2005. Minéralogie des argiles de sols: Structure, altération, réactivité. Habilitation thesis, University of Strasbourg, France.

FAO. 2006. World reference base for soil resources 2006: A framework for international classification, correlation and communication. FAO, Rome.

FAO. 2007. World reference base for soil resources 2006, first update 2007. World Soil Resources Report 103. FAO, Rome.

Finke, P.A. 2012. Modeling the genesis of luvisols as a function of topographic position in loess parent material. Quaternary Int. 265:3–17. doi:10.1016/j.quaint.2011.10.016

Furukawa, Y., J.L. Watkins, J. Kim, K.J. Curry, and R.H. Bennett. 2009. Aggregation of montmorillonite and organic matter in aqueous media containing artificial seawater. Geochem. Trans. 10:2. doi:10.1186/1467-4866-10-2

Gallet, C., and C. Keller. 1999. Phenolic composition of soil solutions: Comparative study of lysimeter and centrifuge waters. Soil Biol. Biochem. 31:1151–1160. doi:10.1016/S0038-0717(99)00033-4

Goldberg, S., and H.S. Forster. 1990. Flocculation of reference clays and arid-zone soil clays. Soil Sci. Soc. Am. J. 54:714–718. doi:10.2136/sssaj1990.03615995005400030014x

Goldberg, S., and R.A. Glaubig. 1987. Effect on saturating cation, pH, and aluminum and iron oxide on the flocculation of kaolinite and montmorillonite. Clays Clay Miner. 35:220–227. doi:10.1346/CCMN.1987.0350308

Grolimund, D., M. Elimelech, and M. Borkovec. 2001. Aggregation and deposition kinetics of mobile colloidal particles in natural porous media. Colloids Surf. A 191:179–188. doi:10.1016/S0927-7757(01)00773-7

Gu, B., and H.E. Doner. 1992. The microstructure of dilute clay and humic acid suspensions revealed by freeze-fracture electron microscopy. Clays Clay Miner. 40:246–250. doi:10.1346/CCMN.1992.0400215

Guan, J., T.D. Waite, and R. Amal. 1998. Rapid structure characterization of bacterial aggregates. Environ. Sci. Technol. 32:3735–3742. doi:10.1021/es980387u

Heath, D., and T.F. Tadros. 1983. Influence of pH, electrolyte, and poly (vinyl alcohol) addition on the rheological characteristics of aqueous dispersions of sodium montmorillonite. J. Colloid Interface Sci. 93:307–319. doi:10.1016/0021-9797(83)90415-0

Hesterberg, D., and A.L. Page. 1990. Critical coagulation concentrations of sodium and potassium illite as affected by pH. Soil Sci. Soc. Am. J. 54:735–739. doi:10.2136/sssaj1990.03615995005400030018x

Hofmann, U. 1961. Geheimnisse des tons. Ber. Dtsch. Keram. Ges. 38:201–207.

Howitt, R.W., and S. Pawluk. 1985. The genesis of a gray luvisol within the boreal forest region. II. Dynamic pedology. Can. J. Soil Sci. 65:9–19. doi:10.4141/cjss85-002

Hubert, F. 2008. Modélisation des diffractogrammes de minéraux argileux en assemblages complexes dans deux sols de climat tempéré. Implications minéralogique et pédologique. Ph.D. diss. Université de Poitiers, France.

Hunter, R.J., 1981. Zeta potential in colloid science: Principles and applications. Academic Press, London.

Jacobsen, O., P. Moldrup, C. Larsen, L. Konnerup, and L. Petersen. 1997. Particle transport in macropores of undisturbed soil columns. J. Hydrol. 196:185–203. doi:10.1016/S0022-1694(96)03291-X

Jarvis, N.J., K.G. Villholth, and B. Ulén. 1999. Modelling particle mobilization and leaching in macroporous soil. Eur. J. Soil Sci. 50:621–632. doi:10.1046/j.1365-2389.1999.00269.x

Johnson, D.W. 1995. Temporal patterns in beech forest soil solutions: Field and model results compared. Soil Sci. Soc. Am. J. 59:1732–1740. doi:10.2136/sssaj1995.03615995005900060032x

Johnston, C.T., and E. Tombacz. 2002. Surface chemistry of soil minerals. In: J.B. Dixon, and D.G. Schulze, editors, Soil Mineralogy with Environmental Applications. SSSA Book Ser. 7, SSSA, Madison, WI. p. 37–67.

Kaplan, D.I., P.M. Bertsch, D.C. Adriano, and W.P. Miller. 1993. Soil-borne mobile colloids as influenced by water flow and organic carbon. Environ. Sci. Technol. 27:1193–1200. doi:10.1021/es00043a021

Keren, R., and D.L. Sparks. 1995. The role of edge surfaces in flocculation of 2:1 clay minerals. Soil Sci. Soc. Am. J. 59:430–435. doi:10.2136/sssaj1995.03615995005900020023x

Kinsela, A.S., A. Tjitradjaja, R.N. Collins, T.D. Waite, T.E. Payne, B.C.T. Macdonald, and I. White. 2010. Influence of calcium and silica on hydraulic properties of sodium montmorillonite assemblages under alkaline conditions. J. Colloid Interface Sci. 343:366–373. doi:10.1016/j.jcis.2009.10.044

Kjaergaard, C., H.C.B. Hansen, C.B. Koch, and K.G. Villholth. 2004. Properties of water-dispersible colloids from macropore deposits and bulk horizons of an agrudalf. Soil Sci. Soc. Am. J. 68:1844–1852. doi:10.2136/sssaj2004.1844

Labille, J., 2003. Déstabilisation d'une suspension colloïdale de montmorillonite par coagulation-floculation, en présence de polysaccharides. Ph.D. thesis, Institut National Polytechnique de Lorraine, France.

Labille, J., F. Thomas, I. Bihannic, and C. Santaella. 2003. Destabilization of montmorillonite suspensions by Ca2+ and succinoglycan. Clay Miner. 38:173–185. doi:10.1180/0009855033820087

Ladouche, B., A. Luc, and D. Nathalie. 2009. Chemical and isotopic investigation of rainwater in Southern France (1996–2002): Potential use as input signal for karst functioning investigation. J. Hydrol. 367:150–164. doi:10.1016/j.jhydrol.2009.01.012

Laegdsmand, M., K.G. Villholth, M. Ullum, and K.H. Jensen. 1999. Processes of colloid mobilization and transport in macroporous soil monoliths. Geoderma 93:33–59. doi:10.1016/S0016-7061(99)00041-5

Lagaly, G. 1989. Principles of flow of kaolin and bentonite dispersions. Appl. Clay Sci. 4:105–123. doi:10.1016/0169-1317(89)90003-3

Lagaly, G. 2006. Chapter 5: Colloid clay science. In: F. Bergaya, B.K.G. Theng, and G. Lagaly, editors, Developments in clay science. Vol. 1. Elsevier, Amsterdam. p. 141–245.

Lagaly, G., and S. Ziesmer. 2003. Colloid chemistry of clay minerals: The coagulation of montmorillonite dispersions. Adv. Colloid Interface Sci. 100–102:105–128. doi:10.1016/S0001-8686(02)00064-7

Lambert, S., A. Thill, P. Ginestet, J.M. Audic, and J.Y. Bottero. 2000. Structural interpretations of static light scattering patterns of fractal aggregates. J. Colloid Interface Sci. 228:379–385. doi:10.1006/jcis.2000.6965

Laubel, A., O.H. Jacobsen, B. Kronvang, R. Grant, and H.E. Andersen. 1999. Subsurface drainage loss of particles and phosphorus from field plot experiments and a tile-drained catchment. J. Environ. Qual. 28:576–584. doi:10.2134/jeq1999.00472425002800020023x

Le Bissonnais, Y. 1996. Aggregate stability and assessment of soil crustability and erodibility: I. Theory and methodology. Eur. J. Soil Sci. 47:425–437. doi:10.1111/j.1365-2389.1996.tb01843.x

Le Bissonnais, Y., A. Bruand, and M. Jamagne. 1989. Laboratory experimental study of soil crusting: Relation between aggregate breakdown mechanisms and crust structure. Catena 16:377–392. doi:10.1016/0341-8162(89)90022-2

Liu, P., T. Kendelewicz, and G.E. Brown, Jr. 1998. Reaction of water with MgO(100) surfaces. Part II: Synchrotron photoemission studies of defective surfaces. Surf. Sci. 412–413:315–332. doi:10.1016/S0039-6028(98)00445-2

Löhr, S.C., and M.E. Cox. 2012. The influence of vegetation and soil type on the speciation of iron in soil water. Eur. J. Soil Sci. 63:377–388. doi:10.1111/j.1365-2389.2012.01435.x

Majdalani, S., E. Michel, L. Di-Pietro, and R. Angulo-Jaramillo. 2008. Effects of wetting and drying cycles on in situ soil particle mobilization. Eur. J. Soil Sci. 59:147–155. doi:10.1111/j.1365-2389.2007.00964.x

Manning, B.A., and S. Goldberg. 1996. Modeling arsenate competitive adsorption on kaolinite, montmorillonite and illite. Clays Clay Miner. 44:609–623. doi:10.1346/CCMN.1996.0440504

Marques, R., J. Ranger, D. Gelhaye, B. Pollier, Q. Ponette, and O. Gœdert. 1996. Comparison of chemical composition of soil solutions collected by zero-tension plate lysimeters with those from ceramic-cup lysimeters in a forest soil. Eur. J. Soil Sci. 47:407–417. doi:10.1111/j.1365-2389.1996.tb01414.x

Mercier, P., L. Denaix, M. Robert, and G. de Marsily. 2000. Caractérisation des matières colloïdales évacuées au cours du drainage agricole: Incidence sur l'évolution pédogénétique des sols. Comptes Rendus Académie Sci. Ser. IIA. Earth Planet. Sci. 331:195–202. doi:10.1016/S1251-8050(00)01403-8

Michel, E., S. Majdalani, and L. Di-Pietro. 2010. How differential capillary stresses promote particle mobilization in macroporous soils: A novel conceptual model. Vadose Zone J. 9:307–316. doi:10.2136/vzj2009.0084

Missana, T., and A. Adell. 2000. On the applicability of DLVO theory to the prediction of clay colloids stability. J. Colloid Interface Sci. 230:150–156. doi:10.1006/jcis.2000.7003

Négrel, P., and S. Roy. 1998. Chemistry of rainwater in the Massif Central (France): A strontium isotope and major element study. Appl. Geochem. 13:941–952. doi:10.1016/S0883-2927(98)00029-8

Penner, D., and G. Lagaly. 2000. Influence of Organic and inorganic salts on the coagulation of montmorillonite dispersions. Clays Clay Miner. 48:246–255. doi:10.1346/CCMN.2000.0480211

Permien, T., and G. Lagaly. 1994. The rheological and colloidal properties of bentonite dispersions in the presence of organic compounds IV. Sodium montmorillonite and acids. Appl. Clay Sci. 9:251–263. doi:10.1016/0169-1317(94)90003-5

Quénard, L., A. Samouëlian, B. Laroche, and S. Cornu. 2011. Lessivage as a major process of soil formation: A revisitation of existing data. Geoderma 167–168:135–147.

Ranger, J., D. Discours, D. Mohamed Ahamed, C. Moares, É. Dambrine, D. Merlet, and J. Rouiller. 1993. Comparaison des eaux liées et des eaux libres des sols de 3 peuplements d'épicéa (Picea abies Karst) des Vosges. Application à l'étude du fonctionnement actuel des sols et conséquences pour l'état sanitaire des peuplements. Ann. Sci. For. 50:425–444. doi:10.1051/forest:19930502

Ranger, J., S. Loyer, D. Gelhaye, B. Pollier, and P. Bonnaud. 2007. Effects of the clear-cutting of a Douglas-fir plantation (Pseudotsuga menziesii F.) on the chemical composition of soil solutions and on the leaching of DOC and ions in drainage waters. Ann. For. Sci. 64:183–200. doi:10.1051/forest:2006103

Ranger, J., R. Marques, and J.-H. Jussy. 2001. Forest soil dynamics during stand development assessed by lysimeter and centrifuge solutions. For. Ecol. Manage. 144:129–145. doi:10.1016/S0378-1127(00)00366-2

Ryan, J.N., and M. Elimelech. 1996. Colloid mobilization and transport in groundwater. Colloids Surf. A 107:1–56. doi:10.1016/0927-7757(95)03384-X

Ryan, J.N., T.H. Illangasekare, M.I. Litaor, and R. Shannon. 1998. Particle and plutonium mobilization in macroporous soils during rainfall simulations. Environ. Sci. Technol. 32:476–482. doi:10.1021/es970339u

Sanusi, A., H. Wortham, M. Millet, and P. Mirabel. 1996. Chemical composition of rainwater in Eastern France. Atmos. Environ. 30:59–71. doi:10.1016/1352-2310(95)00237-S

Schelde, K., P. Moldrup, O.H. Jacobsen, H. de Jonge, D. Jonge, L. Wollesen, and T. Komatsu. 2002. Diffusion-limited mobilization and transport of natural colloids in macroporous soil. Vadose Zone J. 1:125–136. doi:10.2113/1.1.125

Séquaris, J.-M. 2010. Modeling the effects of Ca2+ and clay-associated organic carbon on the stability of colloids from topsoils. J. Colloid Interface Sci. 343:408–414. doi:10.1016/j.jcis.2009.12.014

Shang, J., M. Flury, G. Chen, and J. Zhuang. 2008. Impact of flow rate, water content, and capillary forces on in situ colloid mobilization during infiltration in unsaturated sediments. Water Resour. Res. 44:W06411. doi:10.1029/2007WR006516

Soil Survey Staff. 1998. Keys to soil taxonomy. 8th ed. USDA-NRCS, U.S. Gov. Print. Office, Washington, DC.

Sondi, I., O. Milat, and V. Pravdić. 1997. Electrokinetic potentials of clay surfaces modified by polymers. J. Colloid Interface Sci. 189:66–73. doi:10.1006/jcis.1996.4753

Stichting voor Bodemkaartering. 1965. De Bodem van Nederland: Toelichting bij de Bodemkaart van Nederland schaal 1:200 000. Stichting voor Bodemkaartering, Wageningen.

Swistock, B.R., J.J. Yamona, D.R. Dewalle, and W.E. Sharpe. 1990. Comparison of soil water chemistry and sample size requirements for pan vs tension lysimeters. Water Air Soil Pollut. 50:387–396. doi:10.1007/BF00280637

Thill, A., S. Moustier, J. Aziz, M.R. Wiesner, and J.Y. Bottero. 2001. Flocs restructuring during aggregation: Experimental evidence and numerical simulation. J. Colloid Interface Sci. 243:171–182. doi:10.1006/jcis.2001.7801

Thomas, F., L.J. Michot, D. Vantelon, E. Montarges, B. Prelot, M. Cruchaudet, and J.F. Delon. 1999. Layer charge and electrophoretic mobility of smectites. Colloids Surf. A 159:351–358. doi:10.1016/S0927-7757(99)00291-5

Tombacz, E., and M. Szekeres. 2004. Colloidal behavior of aqueous montmorillonite suspensions: The specific role of pH in the presence of indifferent electrolytes. Appl. Clay Sci. 27:75–94. doi:10.1016/j.clay.2004.01.001

Tournassat, C., M. Bizi, G. Braibant, and C. Crouzet. 2011. Influence of montmorillonite tactoid size on Na–Ca cation exchange reactions. J. Colloid Interface Sci. 364:443–454. doi:10.1016/j.jcis.2011.07.039

Tournassat, C., A. Neaman, F. Villiéras, D. Bosbach, and L. Charlet. 2003. Nanomorphology of montmorillonite particles: Estimation of the clay edge sorption site density by low-pressure gas adsorption and AFM observations. Am. Mineral. 88:1989–1995.

Van Olphen, H. 1977. An introduction to clay colloid chemistry: For clay technologists, geologists, and soil scientists. John Wiley & Sons, New York.

Vendelboe, A.L., P. Moldrup, G. Heckrath, Y. Jin, and L.W. de Jonge. 2011. Colloid and phosphorus leaching from undisturbed soil cores sampled along a natural clay gradient. Soil Sci. 176:399–406. doi:10.1097/SS.0b013e31822391bc

Vrbek, B. 2005. Lysimeter researches in peduncled oak forest of northwest Croatia. Paper presented at: Lysimetrie Im Netzwerk Dynamik Von Ökosystemen. Gumpenštajn, Austria. 4 May–4 June.

Wanner, H., Y. Albinsson, O. Karnland, E. Wieland, P. Wersin, and L. Charlet. 1994. The acid/base chemistry of montmorillonite. Radiochim. Acta 66–67:157–162.

Watmough, S.A., I. Koseva, and A. Landre. 2013. A comparison of tension and zero-tension lysimeter and PRS$^{TM}$ probes for measuring soil water chemistry in sandy boreal soils in the Athabasca Oil Sands Region, Canada. Water Air Soil Pollut. 224:1663. doi:10.1007/s11270-013-1663-5

Wojdyr, M. 2010. *Fityk* : A general-purpose peak fitting program. J. Appl. Cryst. 43:1126–1128. doi:10.1107/S0021889810030499

Chapitre VI

# VI. Conclusion générale et perspectives